Eur Biophys J (1991) 20:293–303

European Biophysics Journal
© Springer-Verlag 1991

Two dimensional diffusion of small molecules on protein surfaces: an EPR study of the restricted translational diffusion of protein-bound spin labels

Heinz-Jürgen Steinhoff, Olaf Dombrowsky, Christine Karim, and Christoph Schneiderhahn

Institut für Biophysik, Ruhr-Universität Bochum, Universitätsstrasse 150, W-4630 Bochum, Federal Republic of Germany

Received July 19, 1991 / Accepted in revised form October 21, 1991

Abstract. Heisenberg spin exchange rates and dipole-dipole spin lattice relaxation rates for deuterated ^{14}N- and ^{15}N-spin labels bound selectively to the histidine *His15* and to the lysines *Lys13*, 96, 97 of the lysozyme molecule have been determined with the aid of electron spin resonance spectroscopy. The results can be interpreted in terms of a two dimensional translational diffusion of the nitroxide tips of the spin labels along the protein surface within restricted surface areas. The spin labels are regarded as models for long amino acid side chains and as probes for the dynamics of protein and water in the vicinity of the protein surface. The translational diffusion coefficient D_{II} is reduced by a factor of between six and thirty compared to the value of D found for the spin labels in bulk water, its value for $T = 295$ K is given by $(1.3 \pm 0.6) \cdot 10^{-10}\,m^2 s^{-1} \geq D_{II} \geq (2.4 \pm 0.3) \cdot 10^{-11}\,m^2 s^{-1}$.

Key words: Protein dynamics – Spin labels – Electron paramagnetic resonance – Translational diffusion – Heisenberg spin exchange – Dipole-dipole interaction

Introduction

Studies of Heisenberg spin exchange and dipole-dipole interactions are well established techniques in electron spin resonance (ESR) for measuring microscopic translational diffusion rates in liquids (Eastman et al. 1969, 1970; Krüger 1972; Percival and Hyde 1976), liquid crystals (Nayeem et al. 1989) and biological membranes (Sachse et al. 1987). Measurements using these methods can provide information leading to enhanced understanding of microscopic molecular behavior.

In this paper, we describe exchange and dipole-dipole interaction studies of translational diffusion rates for bound spin labels on a protein surface. The molecular dynamics of proteins and especially of the protein surface is of considerable interest. The fluctuation of the accessibility of the solvent to charged amino acid side chains modulates the association and dissociation of bound protons and other ions as well as the electric field inside the protein. Such mechanisms may play a role in catalytic processes in enzymes (Warshel 1984). Side chains at the protein surface may open and close active site clefts or the entrance to protein pockets where substrates and ligands bind. Such gating modes control the reactivity of enzymes and proteins (Perutz and Mathews 1966; Case and Karplus 1979). The dynamic properties of the water layers in the vicinity of the protein surface are important for enzymatic activity (Frauenfelder and Gratton 1986). In the present experiments we look at the bound spin labels as models for long amino acid side chains and as probes for the dynamic properties of the protein surface environment (Steinhoff et al. 1989; Steinhoff 1990). The dynamic properties of this probe are investigated and compared to the behavior of free nitroxides in bulk water. Calculations of the spectral densities for dipole-dipole interaction in two dimensional systems, which have recently been developed (Korb et al. 1983, 1984, 1987; Tabony and Korb 1985), and numerical simulations enable us to interpret the results in terms of restricted two dimensional translational diffusion of the nitroxide rings along the protein surface. Upper and lower bounds for the translational diffusion coefficient are given. The findings are discussed in connection with recent results of the diffusional behavior of protein bound water.

Offprint requests to: H.-J. Steinhoff

Experimental

Materials and equipment

Hen egg white lysozyme was obtained from Boehringer Mannheim GmbH. Perdeuterated spin labels N-(1-oxyl-2,2,6,6-tetramethy-4-piperidinyl)iodoacetamide (JAA6) with ^{14}N and ^{15}N isotopes have been synthesized using procedures similar to those given by Gaffney (1976) and Rozantsev (1970). The modification of the histidine *His* 15 (lysozyme(his-JAA6)) was performed by the addition of

a $3 \cdot 10^{-3}$ M solution of lysozyme in phosphate buffer, pH 6.2, to a five fold volume of a $3 \cdot 10^{-3}$ M solution of JAA6 (Wien et al. 1972; Likhtenshtein et al. 1974; Schmidt and Kuntz 1984). The fraction of modified histidine groups after a reaction time of 20 h at $T = 40\,^{\circ}C$ was determined to be 0.93 ± 0.05. A method for the absolute determination of radical concentrations was used (Redhardt and Daseler 1987). The modification of the lysines *Lys* 96, 97 and 13 (lysozyme(lys-JAA6)$_3$) was performed in borate buffer, pH 10, at $T = 40\,^{\circ}C$ (Likhtenshtein et al. 1974; Likhtenshtein 1976). The concentration of lysozyme and JAA6 in the reacting solution was $0.17 \cdot 10^{-3}$ M and $1.7 \cdot 10^{-3}$ M, respectively. After an incubation time of 320 min the number of spin labels bound to one lysozyme molecule was determined to be 2.7 ± 0.2, if the histidine group had previously been blocked by a reduced spin label. Lysozyme samples with less than one spin label molecule bound to the lysine groups (lysozyme(lys-JAA6)$_1$) were prepared by reducing the spin label concentration in the reacting solution by a factor of 10. The samples were freed from unbound spin labels by running through a column of Sephadex G-25. EPR measurements were performed with the modified lysozyme samples in buffered aqueous solution or in buffered glycerol-water mixtures, pH 7. To remove molecular oxygen from the samples several techniques have been applied. Degassing by the freeze-pump-thaw method was difficult to perform in the case of glycerol-water mixtures. Therefore, moistened nitrogen was run through the samples which were then sealed under nitrogen in quartz sample capillaries. Sample capillaries made of teflon (PTFE) (1.1 mm inside diameter) were used in some of the T_1 measurements. A flow of temperature-regulated nitrogen gas over the capillary was used to remove oxygen (Popp and Hyde 1981). The results obtained with these two methods coincided within experimental errors.

EPR absorption spectra were measured on a home made X-band spectrometer equipped with a modified Oxford ESR 9 variable temperature accessory. The modulation frequency was 52 kHz and the modulation amplitude was set to values between 0.5 and $4 \cdot 10^{-5}$ T depending on the line width. The microwave field (B_1) in the cavity was determined according to the method described by Kooser et al. (1969). The microwave power was 0.1 mW ($B_1 = 1.2 \cdot 10^{-6}$ T) unless otherwise stated. The magnetic field B_0 was measured with a Bruker B-NM 12 instrument. After analog to digital conversion the spectra were processed in a personal computer. Saturation recovery transients were measured on a home made pulse EPR spectrometer similar to the scheme given by Huisjen and Hyde (1974) with a bimodal cavity of cylindrical symmetry (Witte 1971). The mode-to-mode isolation is adjusted with reactive paddles. A broadband isolation of 62 dB with quartz dewar and sample can be maintained under standard conditions. The unloaded quality factor Q_0 of each mode was determined to be about 6 500, yielding a ringing time of $\sim 10^{-7}$ s. The power of the detecting field was 1 mW, the saturating pulse with a power of 500 mW was delivered by a TWT (HP1177 H). The transients were amplified by means of a heterodyne amplifier with a voltage gain of 40 dB and recorded by an oscilloscope (Hameg). 10^4 transients were recorded within 6 min and transmitted from the oscilloscope to a personal computer, where the transients are processed. Details of the apparatus and the software are given by Dombrowsky (1990). To reduce possible errors in the determination of T_1 caused by spin exchange and nuclear relaxation the saturating pulse duration was set to 100 μs, which is long compared to the observed relaxation times (Percival and Hyde 1976; Yin et al. 1987). Double exponentials were fitted to the recovery curves (Yin and Hyde 1987; Yin et al. 1988), and T_1 was calculated from the time constant of the slow decay.

Molecular graphics studies and molecular dynamic simulations were performed on a Silicon Graphics IRIS 4D25 workstation using the software Insight I and Discover from Biosym.

The positions of the bound labels

The spin label binding sites of the lysozyme molecule which are modified in this experiment, are the ε-NH-groups of *Lys* 13, *Lys* 96, *Lys* 97 and *His* 15. The time averaged position of the nitroxide ring of the spin label JAA6 bound to *His* 15 is known from NMR measurements (Schmidt and Kuntz 1984). The ring occupies a relatively well defined location in a flat trough near the amino acids *Phe* 3, *His* 15, *Asp* 87 and *Ile* 88. A computer graphics examination shows that the coordinates for the N–O-group are compatible with the position of the spin label ring being in close contact with the protein surface. Significant positions of the nitroxides bound to the lysines are not known. Owing to the greater length and flexibility of the lysine side chains compared to the histidine side chain, a couple of positions of the nitroxide rings with respect to the protein surface may be possible. In spite of this long flexible leg on the labels the rotational correlation times are increased by a factor of 100 compared to the values found for the unbound labels in aqueous solution: From studies of the linewidths according to the methods given by Kivelson (1972) and reviewed by Robinson et al. (1985) we find nearly isotropic reorientational diffusion with $\tau_c = (1.9 \pm 0.3)$ ns and (3.4 ± 0.4) ns for the lysine-bound labels and the histidine-bound labels, respectively, $T = 293$ K. Here the rotational correlation time for lysozyme ((10.0 ± 0.5) ns, $T = 293$ K (Dubin et al. 1971)) has been taken into account and the values of τ_c given above are the rotational correlation times of the residual motion of the spin labels relative to the protein. For JAA6 tumbling freely in aqueous solution we find $\tau_c = (20 \pm 3)$ ps in accordance with the results given by Jolicoeur and Friedman (1971). The increase of τ_c is an indication of a strong interaction of the labels with the protein surface in the case of the lysine-bound labels as well. Indeed, neglecting conformational contributions, the gain in free energy due to hydrophobic interaction is 8 kJ/mol, when the nitroxide ring gets into contact with the protein surface. Here we used the parameters for hydrophobicity given by Chothia (1974) and an area of 0.4 nm^2 for the contact between protein and nitroxide ring. These observations indicate that the nitroxide tips of the lysine-bound labels do not project into the bulk water

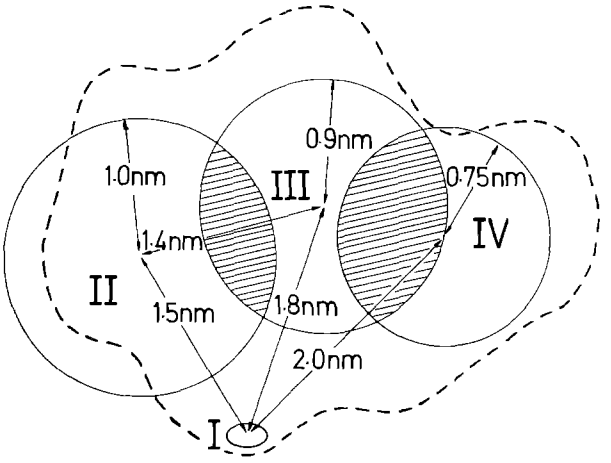

Fig. 1. Projection of the lysozyme molecule with a scheme of the surface areas which are accessible to the N–O groups of bound iodoacetamide spin labels. The roman numbers denote specific binding sites: I, *His* 15; II, *Lys* 13; III, *Lys* 96; IV, *Lys* 97. The figure has been constructed from molecular graphics studies with the assumption that the spin labels II, III and IV and the modified side chains are flexible and the rest of the protein is fixed. Collisions of the nitroxide tips are possible within the overlapping (striped) regions. The circle for I shows the relatively well-defined location of the N–O group of the histidine-bound label according to the experimental data given by Schmidt and Kuntz (1984)

but are in contact with the protein surface, as in the case of the histidine-bound label.

The area on the protein surface which is accessible to the nitroxide tips is evidently restricted by the length of the iodoacetamide part of the label and the flexible part of the lysine side chain. From molecular graphics investigations, where the atoms of the mentioned groups have been flexible and the residual atoms of the lysozyme have been held fixed, we get an indication of these areas as sketched in Fig. 1. The boundaries can be approximated by circles with radius r_l between 0.7 and 1 nm and distances of the centers r_a between 0.9 nm and 1.4 nm. To a first approximation we assume that the distribution of the positions of the N–O-groups within these areas is uniform. In the experimental section it will be shown that this assumption is justified.

The short distance between the bound labels will lead to measurable effects in the ESR spectrum due to dipolar interaction which changes the relaxation times T_1 and T_2. In the case of translational motions collisions in the overlap regions (cf. Fig. 1) will be detectable by means of Heisenberg exchange. These effects will be dominated by the interaction between the label pairs bound to *Lys* 96/97 and *Lys* 96/13, so the following calculations will be performed in terms of a radical pair rather than a radical triplet.

Theory

Dipole-dipole interaction and the dependence of T_1 and T_2 on $D_\parallel$

The investigation of microscopic diffusion mechanisms of small paramagnetic molecules in bulk liquids by the determination of the intermolecular spin lattice relaxation time has been successfully performed in the past (Brändle et al. 1970; Krüger 1969, 1972; Percival and Hyde 1976; Dombrowsky 1990). In contrast to the diffusion of molecules in bulk liquids the diffusive motion of protein bound spin labels is mainly a two dimensional process. The time correlation function of the intermolecular dipole-dipole interaction in two dimensions is significantly different from that in three dimensions (Korb et al. 1983, 1984; Tabony and Korb 1985; Korb et al. 1987). The fundamental equations will be summarized in the following section.

The circular surface areas given in Fig. 1 are approximated by quadratic areas in the following approach. Consider N spins S of the same species diffusing on a finite two dimensional surface of area a^2 in the presence of a strong constant magnetic field. The spin-lattice (T_1) and spin-spin (T_2) relaxation times are given by (Korb et al. 1984)

$$T_1^{-1} = 3\frac{N g^4 \beta_e^4}{a^2 \hbar^2}\frac{S(S+1)}{D_\parallel \delta^2}\sum_{\lambda=1,2}\left[u_\lambda(\alpha) F\left(\frac{\delta}{a}, \lambda\omega_0\tau\right) + v_\lambda(\alpha) G\left(\frac{\delta}{a}, \lambda\omega_0\tau\right)\right] \quad (1)$$

$$T_2^{-1} = 3\frac{N g^4 \beta_e^4}{a^2 \hbar^2}\frac{S(S+1)}{D_\parallel \delta^2}\sum_{\lambda=0,1,2} k_\lambda\left[u_\lambda(\alpha) F\left(\frac{\delta}{a}, \lambda\omega_0\tau\right) + v_\lambda(\alpha) G\left(\frac{\delta}{a}, \lambda\omega_0\tau\right)\right]$$

where $k_0 = 1/4$, $k_1 = 5/2$, $k_2 = 1/4$ and

$$F\left(\frac{\delta}{a}, \lambda\omega_0\tau\right) = 1/\tau_1\left[\sum_{l=1}^{\infty} b_l^2\, \Omega_l(\lambda\omega_0) + 1/2\sum_{l=1}^{\infty}\sum_{k=1}^{\infty} b_{lk}^2\, \Omega_{lk}(\lambda\omega_0)\right] \quad (2)$$

$$G\left(\frac{\delta}{a}, \lambda\omega_0\tau\right) = 1/\tau_1\left[\sum_{l=1}^{\infty} c_l^2\, \Omega_l(\lambda\omega_0)\right] \quad (3)$$

l and k are the orders of the Lorentzians in the two series, $\Omega_l(\omega_0)$ and $\Omega_{lk}(\omega_0)$, which constitute the spectral densities

$$\Omega_l(\lambda\omega_0) = \frac{\tau_1/l^2}{1+(\lambda\omega_0\tau_1/l^2)^2}$$

and (4)

$$\Omega_{lk}(\lambda\omega_0) = \frac{\tau_1/(l^2+k^2)}{1+(\lambda\omega_0\tau_1/(l^2+k^2))^2}$$

The longest correlation time τ_1, corresponding to the mode $l=1$, is

$$\tau_1 = a^2/(2\pi^2 D_\parallel) \quad (5)$$

The other symbols have the following meaning: ω_0 is the Lamor frequency, δ is the distance of closest approach between two spin labels, $D_\parallel$ is the two dimensional translational diffusion coefficient, and α is the angle between the magnetic field and the normal of the plane. $u(\alpha)$ and $v(\alpha)$ are functions of this angle:

$$u_0(\alpha) = (1-3\cos^2\alpha)^2, \quad u_1(\alpha) = \sin\alpha\cos^2\alpha, \quad u_2 = \sin^4\alpha$$
$$v_0(\alpha) = 9\,u_2(\alpha), \quad v_1(\alpha) = u_1(\alpha), \quad v_2(\alpha) = (1+\cos^2\alpha)^2 \quad (6)$$

For a powder sample or a solution, the relaxation times need to be averaged over all possible orientations and the following expressions for $u(\alpha)$ and $v(\alpha)$ are obtained

$$\begin{aligned} &\langle u_0(\alpha)\rangle = 4/5\,,\ \langle u_1(\alpha)\rangle = 2/15\,,\ \langle u_2(\alpha)\rangle = 1/2\,,\\ &\langle v_0(\alpha)\rangle = 9/2\,,\ \langle v_1(\alpha)\rangle = 2/15\,,\ \langle v(\alpha)\rangle = 28/15\,. \end{aligned} \tag{7}$$

The functions b_l, b_{lk} and c_l are the amplitudes of the harmonic modes, $\mathfrak{L}_l$ and $\mathfrak{L}_{lk}$, which are given by the integrals

$$\begin{aligned} b_l &= \delta \int_{\delta}^{\sim 10\,\delta} \frac{g(r)}{r^2} J_0\left(\pi\, l \frac{r}{a}\right) \mathrm{d}r \\ b_{lk} &= \delta \int_{\delta}^{\sim 10\,\delta} \frac{g(r)}{r^2} J_0\left(\pi\,(l^2+k^2)^{1/2} \frac{r}{a}\right) \mathrm{d}r \\ c_l &= \delta \int_{\delta}^{\sim 10\,\delta} \frac{g(r)}{r^2} J_2\left(\pi\, l \frac{r}{a}\right) \mathrm{d}r \end{aligned} \tag{8}$$

Here J_0 and J_2 are zero and second order Bessel functions, respectively, and $g(r)$ is the molecular radial distribution function (Hwang and Freed 1975). For a uniform distribution of spins on the surface of area a^2 the radial distribution function yields $g(r)=1$.

In the present case the labels are bound and this affects the volume excluded by the label. These properties of the present samples have to be accounted for by a modified radial distribution function, $g(r)$, which is calculated in the following section.

The radial distribution function in two dimensions is given by

$$g(r) = \frac{a^2\, n(r)}{2N\,\pi\, r\, \Delta r} \tag{9}$$

where $n(r)$ is the average number of particles within a circular ring of radius r and thickness Δr. For uniform distributions of spins within the accessible circular areas shown in Fig. 1 $n(r)$ is calculated numerically for each spin label pair, II/III and III/IV, as a function of r_l and r_a. The results show that $n(r)$ can be approximated with good accuracy by means of a Gaussian relation. In the range of validity $0.7\ \mathrm{nm} \le r_a \le 1.5\ \mathrm{nm}$ and $0.5\ \mathrm{nm} \le r_l \le 1\ \mathrm{nm}$ we get

$$n(r) = f \cdot \exp\left\{\frac{(r-1.1\, r_a)^2}{2\cdot(0.7\cdot r_l)^2}\right\} \tag{10}$$

and

$$\begin{aligned} g(r) &= \frac{c}{r} \exp\left\{\frac{(r-1.1\, r_a)^2}{2\cdot(0.7\cdot r_l)^2}\right\} \quad \text{for} \quad r > \delta \\ g(r) &= 0 \qquad\qquad\qquad\qquad\qquad\quad \text{for} \quad r \le \delta \end{aligned} \tag{11}$$

f and c are proportionality constants with $c=0.4$ nm for the geometries given in Fig. 1. The mean encounter distance of the N–O-groups δ is determined from molecular graphics to be 0.5 nm.

With the values of $g(r)$ given above, (11), the dependence of T_1 and T_2 on $D_\parallel$ was calculated for two values of the distances between the binding sites of a spin label pair on the lysozyme surface ($r_a=0.9$ nm and $r_a=1.4$ nm). The results for T_1 are given in Fig. 2. Up to a value of $D_\parallel$ of

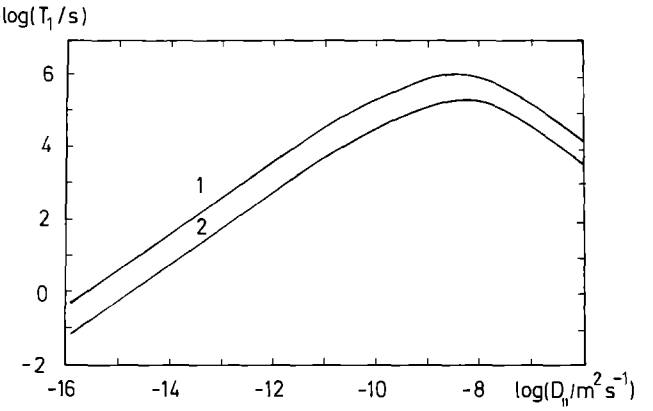

Fig. 2. The relation of the intermolecular spin lattice relaxation rate, T_1^{-1}, to the diffusion coefficient of the restricted two dimensional diffusion, $D_\parallel$. The rates are shown for $r_l = a/2 = 0.7$ nm and two values of the distance r_a of the binding sites: (1) $r_a=0.9$ nm, (2) $r_a=1.4$ nm

$10^{-11}\ \mathrm{m^2/s}$, the relaxation rate T_1^{-1} is proportional to $D_\parallel$. For values of $D_\parallel$ between $10^{-11}\ \mathrm{m^2/s}$ and $10^{-9}\ \mathrm{m^2/s}$ T_1^{-1} is nearly proportional to $D_\parallel^{1/2}$, between $10^{-9}\ \mathrm{m^2/s}$ and $10^{-8}\ \mathrm{m^2/s}$ the curves present a broad maximum. The increase of the distance between the binding sites from 0.9 nm to 1.4 nm decreases the value of T_1^{-1} by a factor of about five in the whole range of $D_\parallel$.

The spin-spin relaxation time T_2 is proportional to $D_\parallel$ for $D_\parallel < 10^{-9}\ \mathrm{m^2/s}$, the range which is of interest here,

$$T_2^{-1} = A/D_\parallel \tag{12}$$

where $A = 0.006\ \mathrm{m^2\ s^{-2}}$ for $r_a=0.9$ nm and $r_l=0.7$ nm for example. The value of A will be discussed further in the experimental section.

Heisenberg spin exchange and its dependence on $D_\parallel$

Heisenberg spin exchange (HE) is known as a phenomenon in which two radicals collide and the two electron spins S_1 and S_2 exchange their nuclear environments. It is a time dependent and diffusion controlled process owing to the relative motion of the radical pairs. During the bimolecular collision, the exchange interaction is described in terms of the Hamiltonian $\mathfrak{H}_{ss}$ (Nayeem et al. 1989):

$$\mathfrak{H}_{ss} = J\, S_1 \cdot S_2 \tag{13}$$

J is twice the exchange integral.

The quantity of interest in the study of HE studies is the spin exchange frequency ω_{HE}. For samples that are not too concentrated, so that the frequency $\omega_{\mathrm{HE}} \ll \gamma\, a_N$, where γ is the electron gyromagnetic ratio and a_N denotes the isotropic hyperfine splitting for the nitroxide spin probes, it has been shown that under strong exchange conditions (i.e., the situation which obtains when the radical pair is sufficiently long lived that the condition $J_0^2\, \tau_1^2 \gg 1$ is fulfilled, τ_1 is the lifetime of the radical pair

and J_0 is the contact value of J) (Eastman et al. 1969, 1970)

$$\omega_{HE} = \tau_2^{-1} = (\sqrt{3}/2)\, f_M\, \gamma\, (\partial_M - \partial_M(0)) = f_M\, \Delta T_2^{-1} \qquad (14)$$

τ_2 means the mean time between successive bimolecular collisions, ∂_M and $\partial_M(0)$ are the first derivative ESR linewidths of the line with spectral index M in the presence and absence of exchange, respectively. M refers to a given hyperfine line in the spectrum, for ^{14}N nitroxides $M = 1, 0, -1$ correspond to the low, central, and high field lines, respectively. f_M is a statistical factor related to the degeneracy of the spin eigenstates. For ^{14}N nitroxide radicals, $f_M = 3/2$ (Nayeem et al. 1989).

For Brownian diffusion in three dimensions, τ_2 is related to the self-diffusion coefficient D of the radicals by (Eastman et al. 1969, 1970; Chandrasekhar 1943)

$$\tau_2^{-1} = 4\,\pi\,\delta\,D\,n \qquad (15)$$

where δ is the mean encounter distance for two radicals undergoing exchange and n is the number density of radicals.

The translational diffusion of the nitroxides on the surface of the protein will be restricted to the surface areas sketched in Fig. 1, owing to the covalent binding of the spin labels to the protein. Collisions between the molecules will be possible only inside the overlapping area parts (cf. Fig. 1). The relation of τ_2 to the diffusion coefficient $D_{\|}$ for the diffusion of the nitroxides along the protein surface cannot be calculated analytically but must be determined by a computer simulation. We use a random walk model for two particles, i.e. two particles perform jumps of length $\lambda < r_l$ and random direction inside the respective accessible surface areas. The diffusion coefficient $D_{\|}$ for translational diffusion in two dimensions is related to λ by (Chandrasekhar 1943)

$$D_{\|} = 1/4\,(\nu/\Delta t)\,\lambda^2 \qquad (16)$$

where ν is the number of jumps within the time interval Δt. For a set of 100 randomly chosen starting positions of the two particles we have determined the mean number of jumps ν' which are necessary for the particles to get closer to each other than the mean encounter distance δ for nitroxide molecules ($= 0.5$ nm). In this case the mean time interval $\Delta t'$ equals the mean time between successive collisions, τ_2. This yields the relation between τ_2^{-1} and $D_{\|}$

$$\tau_2^{-1} = D_{\|}/(1/4\,\nu'\,\lambda^2) \qquad (17)$$

and the change of the relaxation time T_2 with $D_{\|}$ due to Heisenberg exchange is given by

$$\Delta T_{2\,HE}^{-1} = f_M^{-1}/(1/4\,\nu'\,\lambda^2)\, D_{\|} = k\, D_{\|}\,. \qquad (18)$$

The relation of the coefficient k to the distance of the binding sites of the spin labels is given in Fig. 3 for two values of the length of the label.

The equations and values of k given above correspond to the contact exchange model, i.e., that exchange occurs for every bimolecular collision regardless of the relative orientation of the radicals. When the interacting radicals display anisotropic features in their spin exchange, only those collisions for which the colliding radicals are favorably oriented will lead to spin exchange. The measured rate could, therefore, appear smaller than that calculated on the basis of an isotropic exchange model. This situation is discussed in great detail in Nayeem et al. (1989). In the present case the labels are bound. Diffusive motion of the nitroxides within the accessible surface areas may lead to collisions head-on, i.e. with the N–O bonds along the inter-radical axis. This may especially be assumed for collisions of the spin label pair bound to *Lys* 13/96 (cf. Fig. 1) and for the case of closest approach of the histidine bound label to the three other labels. These collisions do not significantly contribute to the exchange integral J (Nayeem et al. 1989). The values of $D_{\|}$ calculated on the basis of the data given in Fig. 3 give, therefore, a lower bound of the present diffusion coefficient.

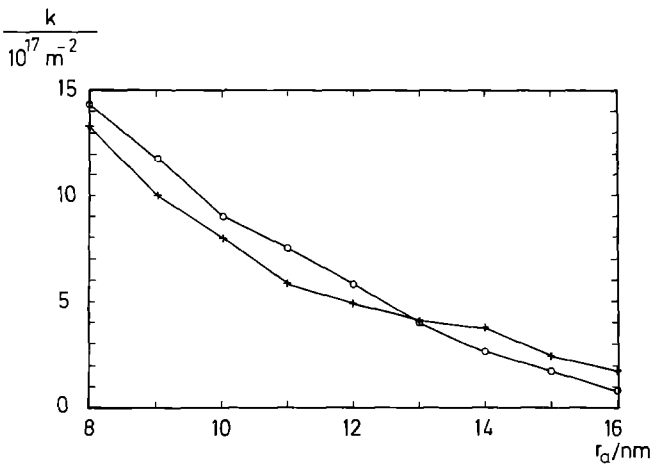

Fig. 3. The proportionality constant k in (18) as a function of r_a for two values of the radius r_l of the surface areas: (o) $r_l = 0.6$ nm and (+) $r_l = 0.7$ nm

A correct measurement of ω_{HE} is possible only when the contribution to the linewidth due to dipole-dipole interaction is taken into account. This was first discussed by Eastman et al. (1969) and more recently by Hyde and Feix (1989) and Nayeem et al. (1989). The dipole-dipole contribution is given by (12) when the relative translational motion of the spin bearing molecules on the protein surface is the only mechanism for the fluctuation of the dipole-dipole interaction. In the range of $D_{\|}$ which is of interest here the contributions of Heisenberg exchange and dipolar relaxation increase with $D_{\|}$ (18) and follow the $1/D_{\|}$ dependence (12), respectively. This property will be used to distinguish dipolar relaxation from Heisenberg exchange. For spin labeled molecules in solution the rotational diffusion of the whole molecule leads to a further averaging of the dipolar broadening, which is difficult to calculate. So an overestimation of $D_{\|}$ results if we determine the diffusion coefficient from the dipole-dipole term alone with the constant of proportionality given in (12). Owing to these difficulties this constant of proportionality, A, will be determined in the experimental section.

Assuming the temperature dependence of D to be Arrhenius-like,

$$D = D_0 \exp(-E_a/\mathrm{RT})\,, \qquad (19)$$

where E_a is the activation energy, the expected temperature dependence of the excess linewidth may be analyzed in terms of the relation (combining Heisenberg exchange term (12), dipolar relaxation term (18))

$$(\sqrt{3}/2)\,\gamma\,[\partial_0 - \partial_0(0)] = \Delta T_2^{-1} = k \cdot D_{\|,0} \exp(-E_a/\mathrm{RT}) + A \exp(E_a'/\mathrm{RT})/D_0' \quad (20)$$

The values with primes are the diffusion parameters, which are contaminated with the rotational diffusion of the whole molecule. The values of $\log(\Delta T_2^{-1})$ will depend linearly on $1/T$ when one of the terms of the sum in (20) dominates. If the Heisenberg exchange term and dipolar relaxation contribute in a similar manner, the function (20) will show a minimum. The excess linewidth $\partial - \partial(0)$ for small values of the microwave field B_1 is determined from measurements of the peak-to-peak derivative linewidth for different values of B_1. The relation between ∂^2 and B_1^2 is given by (Kooser et al. (1969)

$$\partial^2 = \frac{4}{3\,\gamma^2\,T_2^2} + \frac{4}{3}\,\frac{T_1}{T_2}\,B_1^2 \quad (21)$$

The plot of ∂^2 versus B_1^2 delivers T_2 from the intercept.

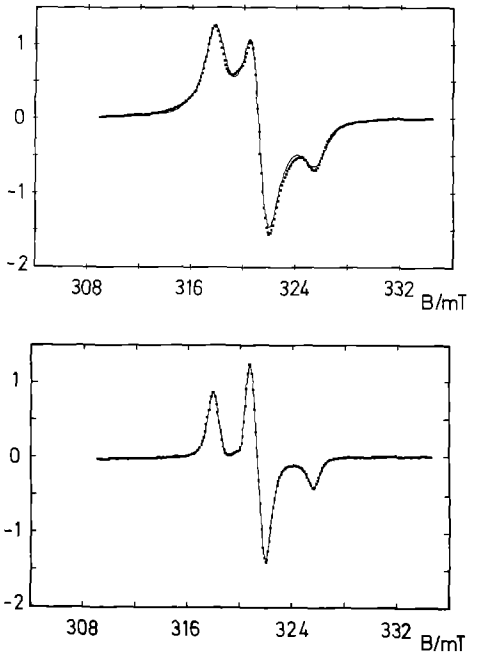

Fig. 4. EPR spectra of lysozyme(*lys*-JAA6)$_3$ (*top*) and lysozyme (*lys*-JAA6)$_1$ (*bottom*) at $T = 152$ K and spectral simulations according to the method described by Steinhoff (1988)

Results and discussion

The distribution of the N–O groups of the lysine-bound labels on the protein surface

For temperatures below $T \approx 200$ K the diffusive motions of the protein matrix are frozen out (Frauenfelder and Gratton 1986) and only small amplitude vibrational motions of the nitroxide rings are detectable (Steinhoff et al. 1989). In this temperature range ESR experiments yield information about the stationary distribution of the N–O group positions on the protein surface. Figure 4 shows ESR spectra for lysozyme(*lys*-JAA6)$_1$ and lysozyme(*lys*-JAA6)$_3$ samples at $T = 152$ K. The lines of the multiple labeled protein are significantly brodenend owing to dipolar interaction. The information about the distribution of the dipoles will be extracted from the linewidth function by means of a computer simulation method. The absorption lines of a pair of interacting spins are shifted by the amount $\pm \Delta B$ from the point without interaction, where ΔB is given to a first approximation by (Abragam 1970; Ciecierska-Tworek et al. 1973)

$$\Delta B = 3\,g\,\beta_e/(8\,r^3)\,(3\cos^2\theta - 1) \quad (22)$$

where θ is the angle between the magnetic field $\boldsymbol{B}_0$ and the distance vector $\boldsymbol{r}$ between the two interacting spins. For powder samples with an isotropic orientation distribution of $\boldsymbol{r}$ and different models for the distribution of $|\boldsymbol{r}|$ the resulting linewidth function $G(\Delta B)$ was simulated. The ESR spectrum $F(B)$ was then calculated by convoluting the spectrum without interaction, $\int f(B')\,\mathrm{d}B'$, with the linewidth function $G(\Delta B) = G(B - B')$

$$F(B) = \int f(B')\,G(B - B')\,\mathrm{d}B' \quad (23)$$

For three models for the distance distribution of the N–O groups, a single distance r, two values of r, and a distribution of r according to (10) with the parameters r_a and r_l, the resulting spectrum $F(B)$ was fitted to the experimental spectrum given in Fig. 4. By far the best correlation between the calculated and measured spectra was achieved when a distribution for r according to (10) was assumed. This calculated spectrum is also shown in Fig. 4. The two fit parameters r_a and r_l were determined to be 1.3 nm and 0.7 nm, in good agreement with the values determined from molecular graphics (cf. Fig. 1). We regard this consistency as evidence for a nearly uniform distribution of the N–O groups on the accessible surface parts of the lysozyme shown in Fig. 1. The values for the radii r_l of the circular areas shown in Fig. 1 are regarded as an upper bound and the experimentally determined value of 0.7 nm is used in the following calculations.

The fit parameters given above do not depend on temperature in the range between 80 K and 200 K. For temperatures above 200 K diffusive motions of parts of the protein surface, including the spin labels, lead to a motional narrowing of the dipolar broadened lines. In this temperature range the translational diffusion behavior of the labels is determined in the next sections using pulse ESR methods and Heisenberg exchange studies.

Determination of $D_{\|}$ from measurements of T_1

The relation of T_1^{-1} to the inverse temperature for lysozyme(*lys*-JAA6)$_1$ and lysozyme(*lys*-JAA6)$_3$ in solutions of two different glycerol-water mixtures is shown in Fig. 5. The relaxation rates increase with increasing temperature in the whole temperature range shown mainly

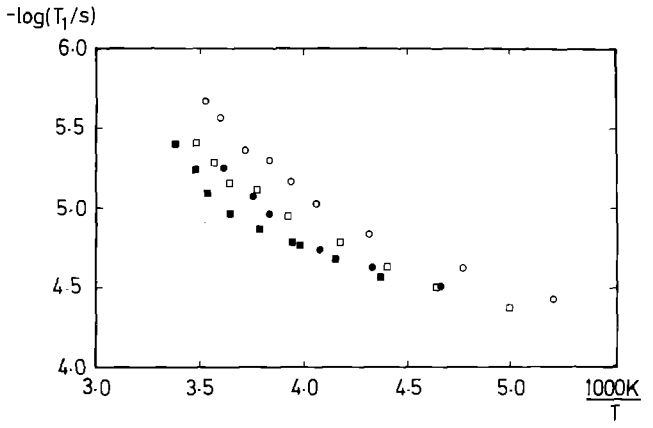

Fig. 5. The relation of the spin lattice relaxation rates to inverse temperature for lysozyme(*lys*-JAA6)$_1$ (closed symbols) and lysozyme(*lys*-JAA6)$_3$ (open symbols) in aqueous solutions of different glycerol concentrations: (o) 64% and (□) 79%

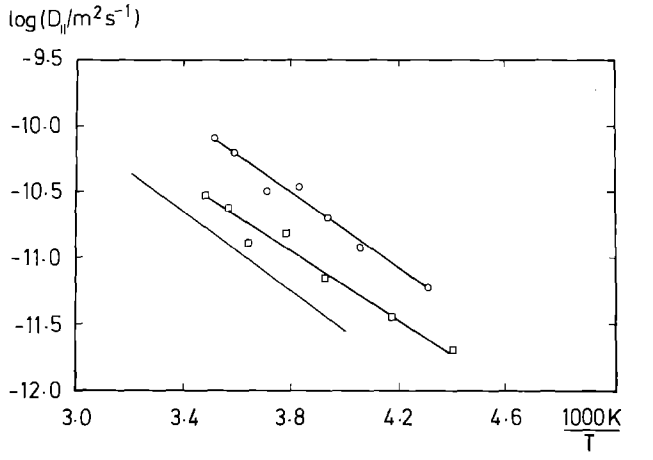

Fig. 6. The diffusion coefficient $D_{\|}$ for the translational diffusion of the nitroxide tips along the protein surface calculated from ΔT_1^{-1}. (o), 64% glycerol-water mixture; (□), 79% glycerol-water mixture, experimental standard error $\sigma_{\log(D_{\|})} \leq 0.1$. The lines are linear regressions to the data points. The line without symbols is the relation of $\log(D_{\|})$ vs T^{-1} determined from Heisenberg spin exchange rates in aqueous solution and calculated for 64% glycerol-water solution

due to the decreasing reorientational correlation times of the nitroxides (Percival and Hyde 1976; Prabhananda and Hyde 1986). Since for a given hyperfine line, temperature, and solution environment, the contribution from intramolecular relaxation is common to both samples, the difference between the experimental determinations of T_1^{-1} is solely due to dipolar interaction of the radicals in the multiple labeled protein. To extract this dipolar component the relation of T_1^{-1} to T^{-1} of the lysozyme(*lys*-JAA6)$_1$ samples is described by an empirical function to interpolate intermediate values. This function is then subtracted from the T_1^{-1} values of the lysozyme(*lys*-JAA6)$_3$ samples. From these rate increments, which are now a function of the dipolar interaction alone, values of the diffusion coefficient $D_{\|}$ are calculated using the calibration curve given in Fig. 2, $r_a = 0.9$ nm. The results are shown in Fig. 6. The plots of $D_{\|}$ versus T^{-1} for the two solutions are well fitted by nearly parallel lines as we would expect for activated diffusion processes. The activation energy E_a determined from the slopes is (26 ± 2) kJ/mol and coincides within experimental error with the value found for the reorientational motion of the lysine-bound labels in glycerol-water solutions, $E_a = (28 \pm 2)$ kJ/mol. This consistency as well as the absence of any significant deviations of the data points from the regression lines in the range of low temperatures are evidence that anything other than motional modulations of the dipole-dipole interaction may be neglected.

The viscosities of the two solutions differ on the average by a factor of five in the temperature range investigated. The relation of the rotational correlation time τ_L of the bound labels JAA6 to the viscosity η in the present range of η, $10\ \text{cP} < \eta < 10^3$ cP, is given by the empirical function $\tau_L \sim \eta^{0.4}$ (Steinhoff 1990). An increase of the viscosity by a factor five without changing the temperature will lead to a doubling of τ_L and, since we assume $\tau \sim D_{\|}^{-1}$, to a decrease of $D_{\|}$ by a factor 0.5. The rotational correlation time of the whole protein, τ_P, is characterized by the Stokes-Einstein formula and, therefore, $\tau_P \sim \eta$. If the modulation of the dipole-dipole interaction of the bound labels due to rotational diffusion of the whole protein were the dominant relaxation mechanism we would expect a proportionality between the determined $D_{\|}$ and η^{-1}. This would result in a decrease of $D_{\|}$ by a factor 0.2, when the viscosity is increased by a factor five. From Fig. 6 we read a factor 0.4 for the ratio of the diffusion coefficients measured in 64% and 79% glycerol-water mixtures at a given temperature. So we conclude that the relative motion of the nitroxide tips on the protein surface is the dominant relaxation process. Slight contributions from the reorientational motion of the whole protein molecule, however, cannot be excluded and lead to an overestimation of the values of $D_{\|}$.

In aqueous solution at $T = 295$ K the rotational correlation times of the bound labels is reduced by 25% compared to the value in 65% glycerol-water mixture. Applied to $D_{\|}$ we get the upper bound of the translational diffusion coefficient of the motion of the spin labels on the protein surface in aqueous solution

$$D_{\|,u}(295\ \text{K}) = (1.3 \pm 0.6) \cdot 10^{-10}\ \text{m}^2\ \text{s}^{-1} \qquad (24)$$

Linewidth measurements

The linewidths of the labeled lysozymes were determined from samples in aqueous solution. Owing to the rapid reorientational motion of the bound spin labels the anisotropy of the tensors g and A is averaged and we get motional narrowed spectra composed of three well separated lines in the case of the ^{14}N-JAA6 and two lines in case of the ^{15}N-JAA6 label. The linewidth ∂ in all cases was greater than $10^7\ \text{s}^{-1}$ so that the hyperfine splitting due to the label methyl deuterons, $a_D = 3.5 \cdot 10^5\ \text{s}^{-1}$ could be neglected (Nayeem et al. 1989) and ∂ and therefore T_2 could be determined according to (21) from the fitting of Lorentzians to the $M = 0$ and $M = 1/2$ lines of the ^{14}N-JAA6 and ^{15}N-JAA6 spectra respectively. This method

has been tested using Freed's slow tumbling program (Freed 1976; Schneider and Freed 1989) and is found to be appropriate for the present samples in the temperature range above 280 K (Steinhoff, unpublished). For temperatures below 280 K the overall rotational correlation times of the bound labels, which is composed of the residual motion of the labels and the rotational diffusion of the lysozyme molecule, exceed 2 ns (3 ns in the case of the histidine bound label) and the spectra have to be fitted using Freed's program. In the present investigation we restrict our investigations to the temperature range above 280 K.

The interaction between ^{15}N-JAA6 bound to His 15 and the lysine-bound spin labels

The $M=1/2$ line of lysozyme(*lys*-JAA6)$_3$(*his*-^{15}N-JAA6)$_1$ is largely contaminated by the wings of the ^{14}N-JAA6 lines. An example of an ESR spectrum of this sample is shown in Fig. 7a. The linewidth cannot be determined directly and we first eliminated the ^{14}N-JAA6 contribution by subtraction of experimental spectra of lysozyme(*lys*-JAA6)$_3$, which had been measured at the same temperatures. Owing to slight differences in the bound spin label concentrations in the two samples the difference spectrum still contains small amounts of the ^{14}N-JAA6 resonance lines. However, the resulting errors in the linewidth determination are now negligible. To decrease the influence of interactions between labels bound to different lysozyme molecules, measurements have been performed with two well known concentrations of lysozyme(*lys*-JAA6)$_3$(*his*-^{15}N-JAA6)$_1$ and the linewidths were extrapolated to zero concentration.

The resulting relaxation rates are shown in Fig. 8. The decrease of the rates with increasing temperature of the samples without intermolecular interaction is due to the decrease of the rotational correlation time τ_L of the nitroxides (Kivelson 1972; Robinson et al. 1985). The correlation times calculated from the linewidth parameters exhibit an Arrhenius-like behavior with an activation energy of (23 ± 2) kJ/mol. However, the linewidth of the $M=1/2$ line of lysozyme(*lys*-JAA6)$_3$(*his*-^{15}N-JAA6)$_1$ is significantly enhanced compared to the values of the single labeled lysozyme(*his*-^{15}N-JAA6)$_1$. The logarithm of the rate increment, $\log(\Delta T_2^{-1}/s^{-1})$, increases linearly with inverse temperature as shown in Fig. 9. Thus, the experimental observation can be completely explained by dipolar interaction as the dominant relaxation mechanism (cf. 20)). The activation energy determined from the slope is $E'_a=(24\pm2)$ kJ/mol and this coincides with the value found for the reorientational motion of the nitroxides on the protein surface. This value, however, is also compatible with the activation energy of the rotational diffusion of the whole protein, which we calculated from the Stokes-Einstein relation and the behavior of the viscosity of water with temperature, $E_a=26$ kJ/mol. Thus, we cannot decide from the slope alone, whether the modulation of the dipole-dipole interaction is mainly due to the relative motions of the nitroxides on the protein surface or to the reorientation of the distance vector be-

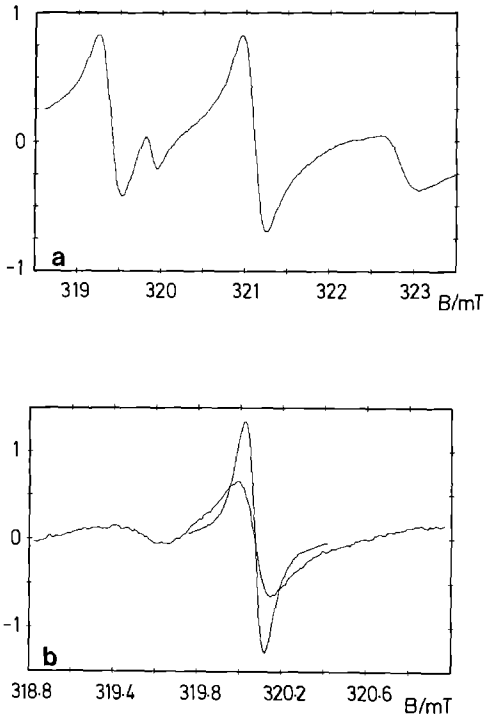

Fig. 7a, b. Cutout of an EPR spectrum of lysozyme(*lys*-JAA6)$_3$(*his*-^{15}N-JAA6)$_1$ in aqueous solution at $T=302$ K. The absorption line at the position $B=319.8$ mT is referred to the low field peak ($M=1/2$) of the ^{15}N-JAA6 spin label. **b** The low field peak of ^{15}N-JAA6 shown in **a** after subtraction of a spectrum of lysozyme(*lys*-JAA6)$_3$ (broad line), and superimposed the same peak for a sample which does not show intermolecular spin-spin interactions, lysozyme(*his*-^{15}N-JAA6)$_1$ (narrow line)

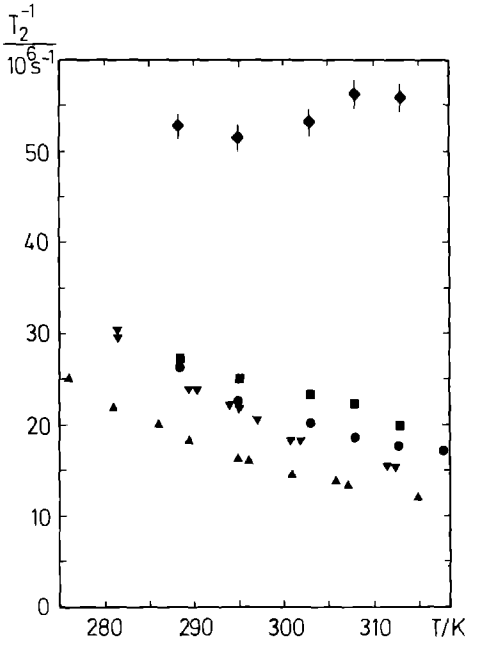

Fig. 8. The spin-spin relaxation rates T_2^{-1} of the $M=0$ and $M=1/2$ absorption lines of the ^{14}N-JAA6 and ^{15}N-JAA6 labels, respectively, for modified lysozymes as a function of temperature: (▲) lysozyme(*his*-^{15}N-JAA6), (▼) lysozyme(*lys*-JAA6)$_3$(*his*-^{15}N-JAA6)$_1$, (●) lysozyme(*lys*-JAA6), (■) narrow component of the absorption line of lysozyme(*lys*-JAA6)$_3$, (◆) broad component of the absorption line of lysozyme(*lys*-JAA6)$_3$

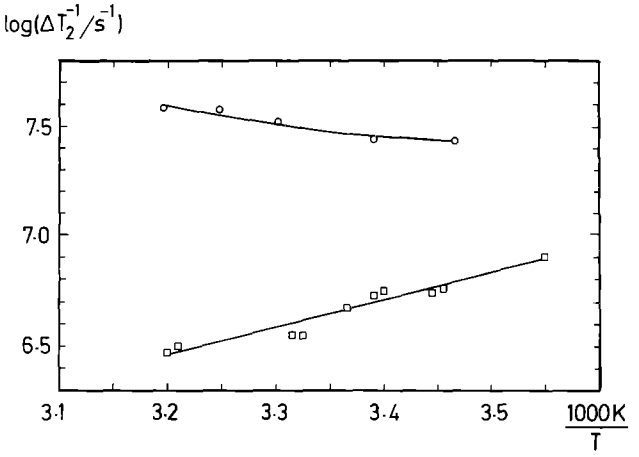

Fig. 9. The rate increment as a function of inverse temperature for ^{15}N-JAA6 in lysozyme (*lys*-JAA6)$_3$(*his*-^{15}N-JAA6)$_1$ (□) and for the JAA6 spin labels in lysozyme (*lys*-JAA6)$_3$ (○). The lines are the best fits of (20) to the data points

tween the nitroxides as a result of the protein rotational diffusion. From the intercept we get the value $D_0/A = (3.4 \pm 0.2) \cdot 10^{-3}$ s. Heisenberg spin exchange interaction for collisions between the histidine-bound spin label and the lysine-bound spin labels is not significant within experimental error. This can be understood in terms of the obvious lack of overlapping parts of the respective accessible surface areas (cf. Fig. 1) and anisotropy of Heisenberg spin exchange (see above).

The interaction of the lysine bound spin labels

The lines of lysozyme (*lys*-JAA6)$_3$ could only be fitted by a superposition of two Lorentzians of different amplitudes and linewidths. The linewidth of the narrow component almost equals the linewidth of the single labeled lysozyme (*lys*-JAA6)$_1$ in the whole temperature range investigated (cf. Fig. 8). This agreement shows that these parts of the spin labels are not influenced by intermolecular interaction. The broad component shows a significantly enhanced linewidth with different temperature behavior compared to that of the other samples. The ratio of the number of spins contributing to each of the two components was determined from double integration of the Lorentzians. The fraction of the narrow part increases from 0.3 ± 0.1 at $T = 288$ K to 0.5 ± 0.1 at $T = 313$ K. From molecular graphics considerations (cf. Fig. 1) we conclude that the probability for significant intermolecular interaction is greater for the label pair bound to *Lys* 96/97 compared to the pair on *Lys* 13/96. So the lines of one third of the labels should be less broadened, in agreement with the experimental results. The experimentally observed increase of the fraction from 0.3 to 0.5 with increasing temperature can be explained if we assume the existence of at least two conformations of the modified lysozyme. One of these conformations has features where the intermolecular interaction of the label pair on *Lys* 96/97 is reduced as well, this state of the protein is mainly occupied at high temperatures.

The relaxation rates of the broad component of lysozyme (*lys*-JAA6)$_3$ increase with increasing temperature in contrast to the behavior of all other samples. This is a first hint that the predominant intermolecular interaction between the labels on *Lys* 96/97 is Heisenberg exchange interaction. The rate increments calculated from the values shown in Fig. 8 are plotted in Fig. 9. Indeed, the slope of the curve is negative in the whole temperature range, so Heisenberg exchange is the predominant line broadening mechanism in this sample (cf. (20)). The experimental data points are well fitted by (20) with parameters $D'_0/A = (3.2 \pm 1.2) \cdot 10^{-3}$ s and $k D_{\|,0} = (2.7 \pm 0.3) \cdot 10^{11}$ s^{-1}. The activation energies E_a and E'_a had been set to the values determined for reorientational diffusion of the labels, 23 kJ/mol, and to the value found for the dipolar term in lysozyme (*his*-^{15}N-JAA6)$_1$, 24 kJ/mol, respectively.

The two values of D'_0/A which characterize the dipole-dipole interaction between the histidine-bound ^{15}N-JAA6 and the lysine bound labels on one side and this interaction between the labels bound to *Lys* 96/97 on the other side coincide, though the accessible surface area and the motional freedom of the histidine-bound label differs from that of the lysine-bound labels (the rotational correlation time of the histidine bound label is twice the mean value for the lysine bound nitroxide rings at a given temperature). So we suppose that the modulation of the dipolar interaction by the rotational diffusion of the whole protein dominates the amount due to the relative motion of the nitroxides on the protein surface in both cases. This is supported by the comparison of the values of $D'_\|$ with the upper bound $D_{\|,u}$, (24). With the distance between the binding sites of 0.9 nm (cf. Fig. 1) we get $A = 0.006$ m^2, this yields $D'_\|$ (295 K) $= (1.2 \pm 0.4) \cdot 10^{-9}$ m^2 s^{-1}. The upper bound of $D_\|$ determined from T_1 measurements was $D_{\|,u}$ (295 K) $= (1.3 \pm 0.6) \cdot 10^{-10}$ m^2 s^{-1}. Thus $D'_\|$ is about ten times the upper bound of $D_\|$ and almost twice the value of D determined for free spin labels in water (The application of the Stokes-Einstein relation with a radius of the spin label of 0.3 nm yields D (295 K) $= 7.2 \cdot 10^{-10}$ m^2 s^{-1}). So the assumption of the rotational diffusion of the whole protein molecule as the main contribution to the dipolar modulation is justified and the dipolar term in (20) cannot be used to characterize the relative motion of the nitroxides on the protein surface in this experiment.

The determination of $D_\|$ from Heisenberg exchange rates

From the fit of (20) to the experimental data points of lysozyme (*lys*-JAA6)$_3$ shown in Fig. 9 one obtains $k D_{\|,0} = (2.7 \pm 0.3) \cdot 10^{11}$ s^{-1}. With a value of $k = 1 \cdot 10^{18}$ m^{-2} taken from Fig. 3 for $r_a = 0.9$ nm and $E_a = 23$ kJ/mol we get the lower bound of $D_\|$

$$D_{\|,lo}\,(259\text{ K}) = (2.4 \pm 0.3) \cdot 10^{-11}\text{ m}^2\text{ s}^{-1} \qquad (25)$$

The values of $D_\|$ determined from Heisenberg exchange and T_1 measurements are in good agreement: The lower and upper bound of $D_\|$ differ by a factor of between three and nine. Compared to the value of D of three dimensional translational diffusion of spin labels in water the value

of $D_{\|}$ for the translational diffusion on the protein surface is reduced at least by a factor six, but not by more than a factor of thirty.

In general, we note that our fits of $\log(\Delta T_2^{-1})$ vs $1/T$ to a sum of two exponentials describing Heisenberg exchange and dipolar contributions to the excess linewidth (cf. 20) and Fig. 9) are reasonable. We found that Heisenberg exchange is the dominant line broadening mechanism for the interaction between the spin label pair bound to *Lys* 96/97. This is in agreement with the results of studies of nitroxide radicals in low viscosity solutions, in membranes and liquid crystals (Eastman et al. 1969; Feix et al. 1984; Hyde and Feix 1989; Nayeem et al. 1989). The authors discussed the contributions of the pseudosecular electron-electron dipolar relaxation and have shown that dipolar contributions are not dominant in those systems. In contrast to this the temperature dependence of the excess linewidth of the $M=1/2$ absorption line of lysozyme(*lys*-JAA6)$_3$(*his*-^{15}N-JAA6) may be explained by dominant dipolar interaction between the spin label bound to *His* 15 and the labels bound to the lysine groups. The known anisotropy of Heisenberg exchange interaction (Nayeem 1989) and steric reasons may lead to a low probability for spin exchange in the case of closest approach of the I/II or I/III spin label pairs (cf. Fig. 1).

Measurements of the diffusional behavior of molecules of dimensions similar to spin labels on protein surfaces are not known to us, so we discuss the above values of $D_{\|}$ in connection with the properties of protein surface water. From NMR experiments of spin labeled bovine serum albumin the translational diffusion of water within the first 1 nm of the protein surface is characterized and the approach yields a value for D of $(3\pm1)\cdot10^{-10}\,m^2\,s^{-1}$ (Polnaszek and Bryant 1984). The diffusion coefficient of water in the vicinity of free nitroxide radicals in aqueous solution was determined to $1.6\cdot10^{-9}\,m^2\,s^{-1}$ in good agreement with other measurements of the self diffusion coefficient of water and the authors conclude that the diffusion coefficient is between five and ten times smaller at the protein surface. On the assumption that the mobility of the nitroxides is reduced by a similar factor our results are in good agreement with the observations on water dynamics.

Conclusions

We have studied the distribution of the N–O groups of lysozyme bound spin labels at the protein surface and the translational diffusion of these groups. Distance measurements by NMR, free energy estimations and determinations of the rotational correlation times of the bound spin labels lead us to the conclusion that the nitroxide rings are preferably in close contact with the protein surface. The amount of dipolar broadening of the EPR lines at low temperatures is in agreement with a model of an uniform distribution of the N–O groups within surface areas, the radii of which are given to a first approximation by the length of the label and the flexible part of the side chain of the modified amino acid. The observed behavior of the dipole-dipole spin lattice relaxation rates and Heisenberg exchange rates can be explained by restricted translational diffusion of the nitroxide tips within these areas. The translational diffusion coefficient $D_{\|}$ determined by means of the two methods mentioned above is given by

$$(1.3\pm0.6)\cdot10^{-10}\,m^2\,s^{-1}\geq D_{\|}\geq(2.4\pm0.3)\cdot10^{-11}\,m^2\,s^{-1}.$$

Hence D is reduced by a factor between 6 and 30 compared to the translational diffusion of the spin label molecules in bulk water.

If we look at the nitroxide ring as a model for small substrates or ligands propagating along the protein surface the value of $D_{\|}$ may be regarded as a first measure for the diffusion coefficient of these molecules in the vicinity of the protein. Another aspect for the application of the results is the effect of gated reactivity of proteins (Lee and Karplus 1987). The bound spin label may be regarded as a model for an amino acid side chain, which may open or close the active site cleft of a protein. Characteristics of the gating modes and the influence of the solvent on these modes may be deduced from our results.

Short-pulse saturation recovery EPR measurements (Yin et al. 1987, 1988) on lysozyme(*lys*-JAA6)$_3$ and lysozyme(*lys*-JAA6)$_3$(*his*-^{15}N-JAA6)$_1$ will give further information on the exchange rates and electron dipolar relaxation and therefore on the proposed diffusion model. Work on this subject is in progress.

Acknowledgement. We would like to thank Professor A. Redhardt for numerous inspiring discussions.

References

Abragam A (1970) The principles of nuclear magnetism. Clarendon Press, London Glasgow New York

Brändle R, Krüger GJ, Müller-Warmuth W (1970) Impulsspektroskopische Untersuchungen der Elektronenspinrelaxation in freien Radikalen. Z Naturforsch 25A:1–11

Case DA, Karplus M (1979) Dynamics of ligand binding to heme proteins. J Mol Biol 132:343–368

Chandrasekhar S (1943) Stochastic problems in physics and astronomy. Rev Mod Phys 15:1–89

Chothia C (1974) Hydrophobic bonding and accessible surface area in proteins. Nature 248:338–339

Ciecierska-Tworek Z, Pong Van S, Griffith H (1973) Electron-electron dipolar splitting anisotropy of a dinitroxide oriented in a cristalline matrix. J Mol Struct 16:139–148

Dombrowsky O (1990) Messungen der longitudinalen Elektronenrelaxationszeit an spinmarkierten Proteinen und niedermolekularen Modellsystemen. Dissertation, Ruhr-Universität, Bochum

Dubin SB, Clark NA, Benedek GB (1971) Measurement of the rotational diffusion coefficient of lysozyme by depolarized light scattering: configuration of lysozyme in solution. J Chem Phys 54:5158–5164

Eastman MP, Kooser RG, Das MR, Freed JH (1969) Studies of Heisenberg spin exchange in ESR spectra. I. Linewidth and saturation effects. J Chem Phys 51:2690–2709

Eastman MP, Bruno GV, Freed JH (1970) ESR studies of Heisenberg spin exchange. II. Effects of radical charge and size. J Chem Phys 52:2511–2522

Feix JP, Popp CA, Venkataramu SD, Beth AH, Park JH, Hyde JS (1984) An electron-electron double-resonance study of interactions between ^{14}N- and ^{15}N-stearic acid spin-label pairs: Lateral diffusion and vertical fluctuations in dimyristoylphosphatidylcholine. Biochemistry 23:2293–2299

Frauenfelder H, Gratton E (1986) Protein dynamics and hydration. Methods Enzymol 127:207–216

Freed JH (1976) Theory of slow tumbling ESR spectra for nitroxides. In: Berliner LJ (ed) Spin labeling theory and applications. Academic Press, New York, pp 53–132

Gaffney BJ (1976) The chemistry of spin labels. In: Berliner LJ (ed) Spin labeling. Theory and applications. Academic Press, New York, pp 183–232

Huisjen M, Hyde J (1974) A pulsed EPR spectrometer. Rev Sci Instrum 45:669–675

Hwang LP, Freed JH (1975) Dynamic effects of pair correlation functions on spin relaxation by translational diffusion in liquids. J Chem Phys 63:4017–4025

Hyde JS, Feix JB (1989) Electron-electron double resonance. In: Berliner LJ, Reuben J (ed) Spin labeling – theory and applications. Plenum Press, New York, pp 305–337

Jolicoeur C, Friedman HL (1971) Effects of hydrophobic interactions on dynamics in aqueous solutions studied by EPR. Ber Bunsen-Gesell 75:248–257

Kivelson D (1972) Electron relaxation in liquids. Selected topics. In: Muus LT, Atkins PW (eds) Electron spin relaxation in liquids. Plenum Press, New York London, pp 213–277

Kooser RG, Volland WV, Freed JH (1969) ESR relaxation studies on orbitally degenerate free radicals. I. Benzene anion and tropenyl. J Chem Phys 50:5243–5257

Korb JP, Torney DC, McConnell HM (1983) Dipolar correlation function and motional narrowing in finite two-dimensional spin systems. J Chem Phys 78:5782–5789

Korb JP, Winterhalter M, McConnell HM (1984) Theory of spin relaxation by translational diffusion in two-dimensional systems. J Chem Phys 80:1059–1068

Korb JP, Ahadi M, Zientara GP, Freed JH (1987) Dynamic effects of pair correlation functions of spin relaxation by translational diffusion in two-dimensional fluids. J Chem Phys 86:1125–1130

Krüger GJ (1969) Magnetische Relaxation durch Translationsdiffusion in Flüssigkeiten. Z Naturforsch 21a:560–565

Krüger GJ (1972) Electron spin relaxation in solutions of organic free radicals. Adv Mol Relax Process 3:235–251

Lee S, Karplus M (1987) Kinetics of diffusion-influenced bimolecular reactions in solution. II. Effects of the gating mode and orientation-dependent reactivity. J Chem Phys 86:1904–1921

Likhtenshtein GI (1976) Spin labeling methods in molecular biology. Wiley, New York London Sydney

Likhtenshtein GI, Akhmedov YD, Ivanov LV, Krinitskaya LA, Kokhanov YV (1974) Investigation of the lysozyme macromolecule by a spin-labeling method. Mol Biol 8:40–48

Nayeem A, Rananavare SB, Sastry VSS, Freed JH (1989) Heisenberg spin exchange and molecular diffusion in liquid crystals. J Chem Phys 91:6887–6905

Percival PW, Hyde JS (1976) Saturation-recovery measurements of the spin-lattice relaxation times of some nitroxides in solution. J Magn Res 23:249–257

Perutz MF, Mathews FS (1966) An X-ray study of azide methaemoglobin. J Mol Biol 21:199–202

Polnaszek CF, Bryant RG (1984) Nitroxide radical induced solvent proton relaxation: Measurement of localized translational diffusion. J Chem Phys 81:4038–4045

Popp CA, Hyde JS (1981) Effects of oxygen on ESR spectra of nitroxide spin-label probes of model membranes. J Magn Res 43:249–258

Prabhananda BS, Hyde JS (1986) Study of molecular motions in liquids by electron spin relaxation: Halogenated p-semiquinone anions in alcohols. J Chem Phys 85:6705–6712

Redhardt A, Daseler W (1987) A new method for absolute determination of radical concentration by EPR. J Biochem Biophys Methods 15:71–84

Robinson B, Thomann H, Beth A, Fajer P, Dalton L (1985) The phenomenon of magnetic resonance: Theoretical considerations. In: Dalton LR (ed) EPR and advanced EPR studies of biological systems. CRC Press, Boca Raton, Florida, pp 11–111

Rozantsev EG (1970) Free nitroxyl radicals. Plenum Press, New York London

Sachse JH, King MD, Marsh D (1987) ESR determination of lipid translational diffusion coefficients at low spin-label concentrations in biological membranes, using exchange broadening, exchange narrowing, and dipole-dipole interactions. J Magn Res 71:385–404

Schmidt PG, Kuntz ID (1984) Distance measurements in spin-labeled lysozyme. Biochemistry 23:4261–4266

Schneider DJ, Freed JH (1989) Calculating slow motional magnetic resonance spectra. In: Berliner LJ, Reuben J (ed) Spin labeling – theory and applications. Plenum Press, New York, pp 1–76

Steinhoff HJ (1988) A simple method for determination of rotational correlation times and separation of rotational and polarity effects from EPR spectra of spin-labeled biomolecules in a wide correlation time range. J Biochem Biophys Methods 17:237–248

Steinhoff HJ (1990) Residual motion of hemoglobin-bound spin labels and protein dynamics: viscosity dependence of the rotational correlation times. Eur Biophys J 18:7–62

Steinhoff HJ, Lieutenant K, Schlitter J (1989) Residual motion of hemoglobin-bound spin labels as a probe for protein dynamics. Z Naturforsch 44c:280–288

Tabony J, Korb JP (1985) Interpretation of proton N.M.R. spin lattice relaxation time minima in heterogeneous systems by the effects of bounded two dimensional diffusion. Comparison with neutron scattering measurements. Mol Phys 56:1281–1305

Warshel A (1984) Dynamics of enzymatic reactions. Proc Natl Acad Sci USA 81:444–448

Wien RW, Morrisett JD, McConnell HM (1972) Spin-label-induced nuclear relaxation. Distances between bound saccharides, histidine-15, and tryptophan-123 on lysozyme in solution. Biochemistry 11:3707–3716

Witte A (1971) Induktionsanordnung in the ESR-Spektroskopie, Dissertation, Ruhr-Universität, Bochum

Yin JJ, Hyde JS (1987) Application of rate equations to ELDOR and saturation recovery experiments on ^{14}N: ^{15}N spin-label pairs. J Magn Res 74:82–93

Yin JJ, Pasenkiewicz-Gierula M, Hyde JS (1987) Lateral diffusion of lipids in membranes by pulse saturation recovery electron spin resonance. Proc Natl Acad Sci USA 84:964–968

Yin JJ, Feix JB, Hyde JS (1988) Solution of the nitroxide spin-label spectral overlap problem using pulse electron spin resonance. Biophys J 53:525–531